

Upgrade of the ATLAS MDT Readout and Trigger for the HL-LHC

Robert Richter* †

Max-Planck-Institute for Physics, Munich

E-mail: Robert.Richter@cern.ch

The luminosity increase at the LHC in Phase-II calls for an in-depth redesign of the Monitored Drift Tube (MDT) chamber readout. One reason for this is the high rate of primary detector signals which requires increased readout bandwidth all along the data path. The second reason is due to a new concept for the formation of the Level-1 muon trigger (L1), which aims to improve the selectivity for muons with high transverse momentum (p_T). While in the present system the L1 trigger is exclusively based on specialized trigger chambers (RPC in the barrel, TGC in the endcap), which deliver tracking information with very limited accuracy, the L1 trigger will, in Phase-II, also consider tracking information from the MDT: the time resolution of the trigger chambers, able to tag the beam crossing (BX), will be combined with the high spatial accuracy of the MDT.

In the new L1 trigger scheme, the selection of MDT hits corresponding to a given BX, will be based on a Region of Interest (RoI) provided by the trigger chambers. Considering only MDT hits in the RoI will result in a large reduction of the relevant data volume. The selected MDT hits will be tested for consistency with the track direction, as defined by the RoI. If confirmed, the MDT hits are used for a better p_T definition.

The rate of background hits from γ and neutron conversions is several orders of magnitude higher than the one from muon hits. The selection of muons against this background ("hit extraction") requires high-speed processing power, capable to supply the relevant information to the Muon Central Trigger Processor (MUCTPI) inside the latency of 10 μ s.

Topical Workshop on Electronics for Particle Physics TWEPP2019

2-6 September 2019

Santiago de Compostela - Spain

*Speaker.

†On behalf of the ATLAS Collaboration.

1. Introduction

The increase of luminosity at the LHC in Phase-II by a factor 7 w.r.t. the original design luminosity of $10^{34} \text{ cm}^{-2} \text{ s}^{-1}$ represents a big challenge for the readout of all ATLAS subdetectors as the readout bandwidth must be increased by nearly an order of magnitude.

Due to the necessity to include MDT data in the L1 trigger, the present readout mode, where only MDT hits from *triggered* beam crossings are retained, had to be abandoned in favour of a mode where *all* hits recorded in the MDT tubes are transferred to the L1 trigger logics and to the back-end electronics. This allows to use the high spatial accuracy of the MDT in the L1 trigger decision, opening a new opportunity to improve trigger selectivity for high- p_T tracks.

Details of the new Trigger and Data Acquisition architecture (TDAQ) and of the Muon Spectrometer readout in Phase-II are given in Ref. [1] [2] and [3] [4], respectively.

2. Selectivity of the Muon Trigger for high- p_T Muons

The total inelastic cross section in p-p collisions at LHC energies is about 88 mb, while the cross section for muons reaching the muon detector, i.e. muons with $p_T > 4 \text{ GeV}$, is only a few μb - roughly 4 orders of magnitude less. Among these muons, the fraction of high- p_T muons, i.e. with a transverse momentum above 20 GeV, is only 40 nb.

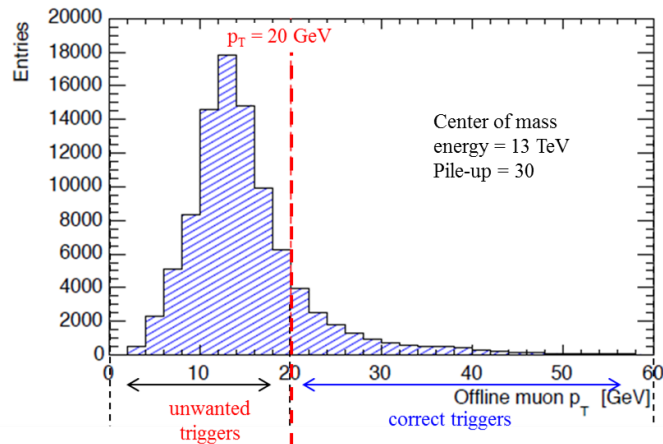


Figure 1: Off-line distribution of muons identified by the L1 trigger at a p_T threshold of 20 GeV [1]

Muons with high- p_T are frequently decay products of heavy particles like Z, W, tt or exotics, and thus belong to a class of interesting physics event signatures. Therefore, high- p_T muons need to be identified at an early stage, rejecting those below the 20 GeV threshold, which are mostly coming from decays of heavy quarks or π/K in hadronic showers.

The selectivity of the present muon trigger was tested when the "real" p_T of triggered high- p_T tracks was reconstructed off-line. In the off-line analysis, information from MDT chambers, from the Inner Detector and from accurate magnetic field maps along the trajectory are available for a precise measurement of the muon track. Fig. 1 shows that the large majority of muons triggered at Level-1 was, in fact, below the critical threshold.

26 The reason for this lack of accuracy at the trigger level is the limited spatial resolution of the
 27 trigger chambers, RPC in the barrel and TGC in the endcap. The p_T measurement of both chamber
 28 types is based on readout strips, perpendicular to the bending plane, with strip widths of 3–6 cm.
 29 As the sagitta of a 20 GeV track is of the order of 1 cm, the actual p_T can only be determined in an
 30 approximate way, insufficient for a sharp p_T threshold.

31 3. Using MDT Coordinates for better p_T -selection

32 In the Muon Spectrometer each trigger chamber is matched to a MDT precision chamber,
 33 which measures the track coordinates with an accuracy of about 0.1 mm. In the barrel, e.g., three
 34 layers of MDT and RPC are arranged in projective towers (see ref. [3]), such that most tracks with
 35 small curvature ("nearly straight") are enclosed inside *one* tower, simplifying the determination of
 36 p_T . Due to the combination of MDT and trigger chamber measurements at the L1 trigger level, fore-
 37 seen in Phase-II, a more accurate p_T determination and a considerable reduction of sub-threshold
 38 triggers will be achieved.

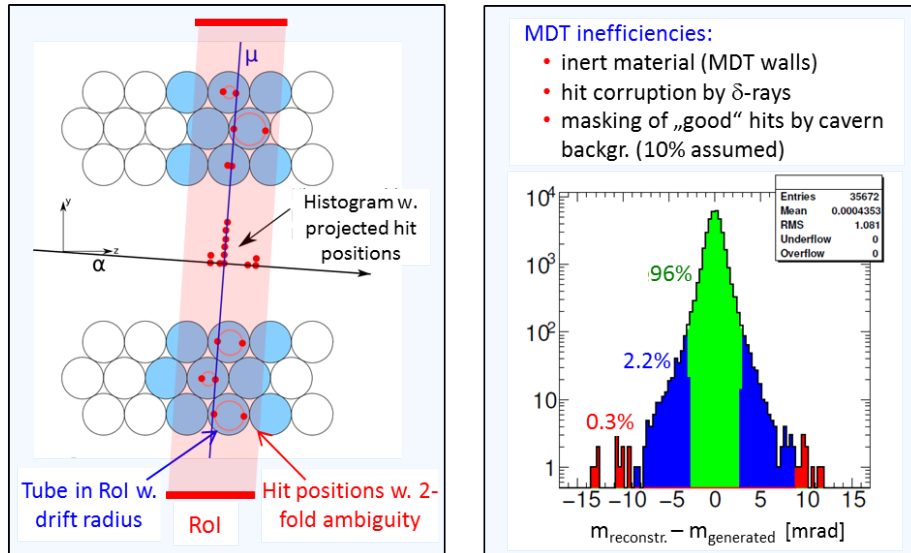


Figure 2: The histogramming method (left) and the resulting efficiency (right).

39 This requires an additional processing step in the generation of the L1 trigger, whereby the
 40 trigger chambers will be used to indicate beam crossing time (BX) and the approximate location
 41 of a trigger candidate, called Region of Interest (RoI), while the MDT hits are used for an accurate
 42 definition of the track coordinates. First, a track segment in each MDT chamber is derived from the
 43 hits in the RoI. Subsequently, the track segments of three MDT/RPC pairs are combined, resulting
 44 in an accurate p_T . This way, most sub-threshold trigger candidates can be suppressed.

45 Fig. 2 (left) illustrates the matching method between the RoI and the MDT hit candidates. A
 46 histogram is filled by projecting all MDT hits onto a plane perpendicular to the direction of the
 47 RoI. The maximum in the histogram denotes the most likely candidate for the muon track segment
 48 in the given RoI. This method automatically discards fake hits caused by the left-right ambiguity
 49 of MDT measurements as well as uncorrelated hits from n/γ -conversion, which in some regions of

50 the detector may reach occupancies of up to 10 %. Once the relevant MDT hits identified, a χ^2 -test
 51 is performed for this track segment. The three track segments inside a trigger tower are finally
 52 combined to determine the track curvature and p_T .

53 The right side of Fig. 2 shows the result of a simulation which takes into account the most im-
 54 portant deteriorating effects for track identification, like δ -electrons, inefficiencies due to hits from
 55 n/γ conversion or due to tracks passing through inert material. The distribution is described by a
 56 gaussian with a small admixture of non-gaussian tails. It shows that about 96 % of the track can-
 57 didates are *correctly* identified, which we define as the difference of slopes between the simulated
 58 and reconstructed track to be $\leq 3\sigma$.

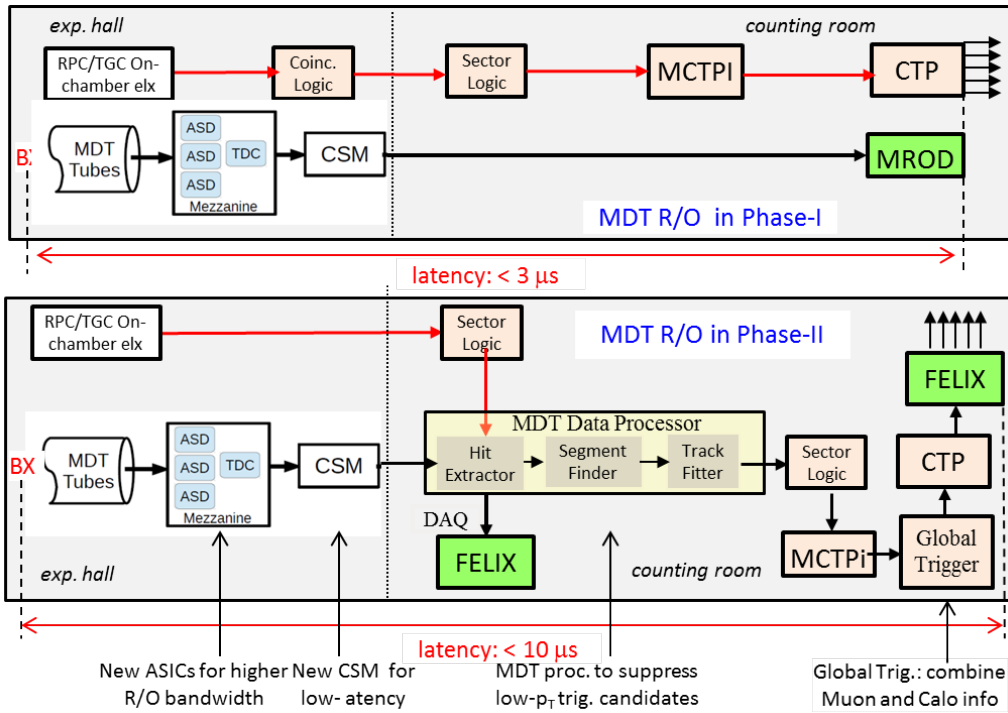


Figure 3: Architecture of the present (top) and future (bottom) readout of the Muon system.

59 4. Technical Implementation

60 Fig. 3 shows the present and future readout architecture. In the present scheme (top), MDT and
 61 RPC/TGC data follow an independent readout path during the L1 latency. In Phase-II (bottom), the
 62 MDT Data Processor collects data from both data streams and only allows L1 trigger candidates
 63 with p_T above 20 GeV, as confirmed by MDT tracking, to be forwarded to the MUTCPI and further
 64 to the Global Trigger.

65 The left part of the figure also shows that the structure of the on-chamber readout of the
 66 MDT is retained in Phase-II. Due to the requirement of higher readout bandwidth and trigger rate,
 67 however, new ASICs had to be developed. The first element in the readout chain, the Amplifier-
 68 Shaper-Discriminator (ASD) showed better performance than the legacy one (Agilent 500 nm),
 69 w.r.t. peaking time, threshold dispersion among the 8 channels and noise. The mismatch of analog

70 parameters (gain, peaking time) among the 8 channels and between different chips was at the level
71 of 1–2%. The yield of good chips, obtained in the engineering run, is above 98%.

72 The TDC has been redesigned for faster readout towards the next stage and for reduced la-
73 tency. The latter is achieved by assigning a separate derandomizing buffer to *each* channel, while
74 there was only one common buffer for all 24 channels in the legacy device. Prototype TDC chips
75 confirm the simulated performance. A second prototype with only minor modifications, serving as
76 production prototype, has already been submitted.

77 The CSM design (Chamber Service Module) is based on the lpGBT readout scheme and does
78 not contain radiation sensitive components like FPGAs. Table 1 shows the main components in the
79 MDT readout chain, where new hardware will be installed.

Component	Function	#	Technology	Main Perf. Criteria
ASD	8-ch ASD	60 k	GF 130 nm	Thresh. dispersion, ENC
TDC	serv. 3 ASDs	20 k	TSCM 130 nm	Transmission rate, latency
CSM	serv. 18 TDCs	1.5 k	lpGBT	Latency, data integrity
Trig. proc.	serv. 3 CSMs	500	FPGA, Zynq	Latency, processor speed

Table 1: New components of the MDT readout

80 5. Filtering of the Muon Trigger at the MUCTPI and Global Trigger

81 While each Sector Logic (SL) module controls only a small angular range in η and ϕ , the
82 MUCTPI, collecting the information of all SL units, may discover more than one muon trigger
83 candidate in barrel or endcap. The presence of two muons in a given BX ("di-muon events"), is
84 often caused by decays of heavy vector mesons like Φ , J/Ψ and Υ . As $\mu\mu$ -decays of particles with
85 known mass are instrumental for detector calibration, the MUCTPI accepts di-muon triggers, if the
86 p_T of at least one of them is above a threshold (e.g. 10 GeV), lower than the single muon threshold
87 of 20 GeV. Selecting di-muon triggers, the MUCTPI has to suppress fake candidates, caused by
88 double counting due to the overlap in Φ of adjacent trigger chambers.

89 At the next level of trigger refinement, the Global Trigger, muon and calorimeter trigger can-
90 didates are compared w.r.t. their relative angle. If the angular separation between a jet and a muon
91 is below a critical value, the L1 trigger will be suppressed, as the muon was, most likely, produced
92 by a heavy quark decay or by an in-flight decay of a shower particle (π/K).

93 At the level of the CTP, prescaling may be implemented, if required by the trigger menu. The
94 final L1 decision is sent to FELIX, from where the trigger is broadcast to all detector frontends.

95 6. Efficiency of the L1 Muon trigger in Phase-II

96 Fig. 4 shows the expected trigger rates for single muons in Phase-II as a function of η . The
97 top distribution (white), corresponds to the present L1 architecture. The middle distribution (blue)
98 shows the expected rates due to the MDT trigger processor. The bottom distribution (green) shows
99 the rates after full off-line reconstruction of the muon p_T . In the middle distribution, one observes
100 two peaks of false triggers at the overlap region between barrel and endcap ($|\eta| \simeq 1.7$).

101 In this region, muon tracks are passing through the magnetic fields of both, barrel and endcap
 102 toroids, providing an inhomogeneous local magnetic field, which results in considerable uncertain-
 103 ties for p_T . Off-line analysis, in contrast, has detailed magnetic field maps at its disposition, and
 104 can, equally important, match muon spectrometer tracks with the corresponding track in the Inner
 105 Detector.

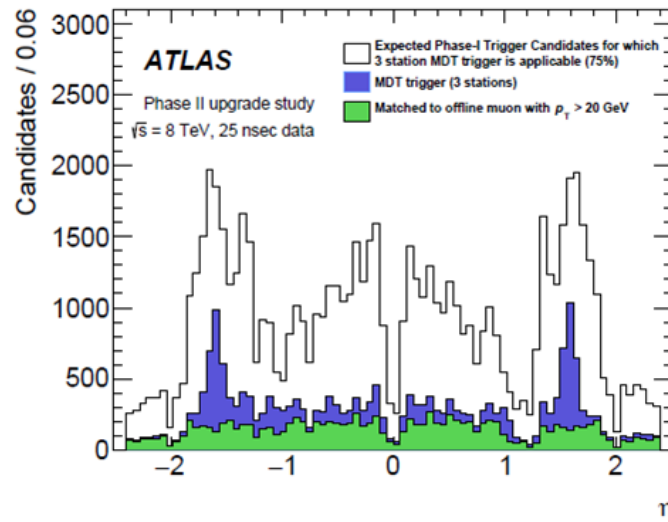


Figure 4: The efficiency of the L1 trigger compared to the off-line analysis [1].

106 7. Conclusions

107 The combination of trigger and precision chamber information will reduce the L1 muon trigger
 108 rate by about a factor of four. From the 1 MHz L1 rate in Phase-II, only about 38 kHz will be used
 109 by the single and about 10 kHz by the di-muon trigger, while in Phase-I these numbers were 15
 110 and 5 kHz, only a factor two higher than in Phase-I, while the luminosity will increase by a factor
 111 of about 7.

112 The new readout architecture requires a complete replacement of the readout chains of MDT
 113 and trigger chambers as well as the installation of new processors for the formation of the combined
 114 trigger. Tests of fully functional prototypes of all components are presently under way. Critical
 115 performance figures are: sustained data rates, bit error rates, latency, power requirements and cost.

116 References

- 117 [1] The ATLAS Collaboration, *TDR for the Phase-II Upgrade of Trigger and DAQ*,
 118 ATL-COM-DAQ-2017-185, Dec. 2017
- 119 [2] The ATLAS Collaboration, *TDR for the Phase-II Upgrade of the ATLAS Muon Spectrometer*,
 120 CERN-LHCC-2017-017, ATLAS-TDR-026-2017
- 121 [3] The ATLAS Collaboration, *The ATLAS Experiment at the CERN Large Hadron Collider*, *JINST* **3**
 122 S08003 (2008)
- 123 [4] Y. Arai et al., *ATLAS Muon Drift Tube Electronics*, *JINST* **3** P09001 (2008)